OXIDATION AND HYDROGEN PICKUP PROPERTIES OF ZIRCALOY CLADDING UPON DEPOSITION OF PLATINUM NANOPARTICLES IN BOILING WATER REACTOR ENVIRONMENT

SRIHARITHA ROWTHU*, PASCAL V. GRUNDLER, STEFAN RITTER
Paul Scherrer Institut (PSI), Laboratory for Nuclear Materials, Nuclear Energy and Safety Division, CH-5232 Villigen, Switzerland

BRITTA HELMERSSON, LENA OLIVER
Westinghouse Electric Sweden AB, 72163 Västerås, Sweden

*Corresponding author: sriharitha.rowthu@psi.ch

ABSTRACT

To extenuate stress corrosion cracking (SCC) in several components of boiling water reactors (BWRs), Pt nanoparticles are deposited onto them in-situ, by hydrolysis and condensation of $Na_2Pt(OH)_6$ solution injected into the reactor feed water stream. These Pt particles catalyse the reduction reaction of O_2 and H_2O_2 in the presence of stoichiometric excess of H_2 gas, which results in the reduction of electrochemical corrosion potentials. Nevertheless, these Pt particles, which are also deposited on Zircaloy fuel cladding surfaces, were hypothesized to possibly enhance its hydrogen pickup and corrosion rate. Consequently, an initial waiting time (several weeks) was recommended between the installation of new fuel elements and injection of $Na_2Pt(OH)_6$ solution, to allow sufficient growth of protective Zircaloy surface oxide. However, such a waiting time may be critical to some components susceptible to SCC and keeping it to a minimum is thus highly desirable.

At PSI, the oxidation and hydrogen pickup properties of Zircaloy-2 cladding tubes in simulated BWR environment have been investigated by varying the initial waiting time prior to Pt application. The total test duration was kept constant to 60 days during all the experiments. Electron microscopy evaluations of Pt-treated Zircaloy-2 surfaces revealed no major variation in the ZrO_2 thickness on the cladding surfaces when the waiting time was decreased from 25 to one day. Subsequent hot gas extraction measurements revealed hydrogen pickup contents by the Zircaloy-2 substrates in a comparable range. At this stage it can be summarized that no major detrimental effects due to Pt deposition were observed for the investigated Zircaloy-2 cladding both, in terms of oxidation and hydrogen pickup properties. Nevertheless, further long-term tests would be needed to confirm this observation.

1. Introduction

Stress corrosion cracking (SCC) has been identified as a major concern for the structural integrity of boiling water reactor (BWR) components worldwide [1]. Typical structural materials are austenitic stainless steels, nickel-base alloys and low-alloy steels [2]. Reactor water undergoes radiolysis and unequal liquid-steam partitioning generates a stoichiometric excess of O_2 and H_2O_2 in the liquid and thus results in a highly oxidizing environment. Under the operating conditions of a BWR, of ~72 bar and temperatures of ~270 - 288 °C, these oxidizing species have led to high electrochemical corrosion potentials (ECPs) inducing a high susceptibility to SCC [1]. To lower the ECP and thus extenuate SCC, the use of noble metals (Pd, Pt, Rh) was first proposed by Niedrach [3] and a deposition technology subsequently developed by General Electric-Hitachi [4, 5]. This technology is referred to as Noble Metal Chemical Addition (NMCA). In combination with hydrogen gas injected into the reactor feed water stream, the so called hydrogen water chemistry (HWC) [6], these noble metals act as catalysts to efficiently reduce the oxidizing species in the presence of excess H_2 [1, 7]. In particular, Pt nanoparticles are now primarily used as catalysts and are obtained

by hydrolysis and condensation reactions of $Na_2Pt(OH)_6$ solution directly injected in the reactor feed water during operation at full power (online NobleChem^{TM} or OLNC) [8, 9]. These Pt nanoparticles deposit on all the water wetted interfaces, of which 30-40 % are Zircaloy fuel cladding surfaces [10]. It has been a persistent concern that these Pt particles may adversely influence the oxidation and hydrogen pickup properties of Zircaloy cladding, especially when fresh fuel elements are installed. There are limited works available addressing this problem [11-13], while only short-term tests (up to 200 h) were conducted. Few minor evidences were found on a positive influence of Pt deposition on the oxidation and hydrogen uptake properties below a certain Pt surface coverage under HWC conditions [11], but those results were not conclusive for implementation in BWR plants.

Meanwhile, EPRI (Electric Power Research Institute) has recommended to inject Pt solution after waiting for 90 days post installation of new fuel elements to allow sufficient growth of a protective passive zirconium oxide layer [14]. However, such long waiting periods could be detrimental to the SCC mitigation influence on other internal components. In this context it is worth mentioning that the nuclear power plant Leibstadt (KKL, Switzerland) is performing its first Pt injection during a plant cycle only 60-70 days after start-up. The rationale behind this being that they have decided, based on results from the research project NORA ("Noble metal deposition behavior in BWRs"), to spread the total amount of Pt to be injected per cycle over more than one injection session in order to counteract erosion of Pt from the surfaces of the plant components maintaining low ECPs for as long as possible. There is also the requirement that the last Pt injection should take place no later than four weeks before end of the cycle to avoid excessive Co-60 release before the outage. To increase the available time span for the multiple injections they have decided to go below the initial 90 days waiting time. So far, no detrimental effects on the Zircaloy cladding have been observed during pool side inspection (appearance, oxide thickness) compared to 90 days pre-injection waiting time [personal communication]. There are ongoing discussions among utilities, fuel manufacturer and regulators to even further reduce this waiting time. Therefore, detailed investigations are needed to further understand the influence of Pt nanoparticle deposits on the oxidation and hydrogen pickup properties of Zircaloy-2 cladding in the early days of its exposure to high-temperature water. This may enable optimization of the waiting period without compromising on the fuel element's functionality.

Therefore, at PSI, in the framework of the NORA project, the influence of Pt nanoparticles on the behaviour of Zircaloy-2 surfaces exposed to simulated BWR conditions (without radiation) is currently investigated. Earlier, results of shorter (25 days) tests [15] have been presented. The current article describes the outcomes from longer (60 days) tests to realize possible effects of Pt deposition on the fuel cladding behaviour on a longer time scale.

2. Experimental details

2.1. Materials: Specimens are classified into three categories based on their composition and geometry. The first type of specimens are cylindrical hollow tubes (ℓ = 74 mm, OD = 9.84 mm, ID = 8.63 mm) closed at one extremity with a TIG-welded solid Zircaloy plug. A cartridge heater has been placed inside these specimens to achieve boiling at their outer surfaces. The connection to the autoclave lid is made with stainless steel Swagelok fittings. The second type of specimens are shorter cylindrical hollow Zircaloy-2 tubes (ℓ = 12 mm, OD = 9.84 mm, ID = 8.63 mm). Both types are made from Zircaloy-2 LK3 Liner tube Optima3 obtained from Westinghouse Electric Sweden AB. The chemical composition of Zircaloy-2 ingot as received from the manufacturer is listed in Table 1. Additionally, some trace elements below 10 ppm are present and the remaining quantity is Zr. The third type of specimens are cuboidal ($13\times10\times4$ mm^3) and made from stainless steel AISI 304L grade.

Table 1. Chemical composition of the Zircaloy-2 ingot obtained from Westinghouse Electric Sweden AB.

Element	**Sn**	**Fe**	**Cr**	**Ni**	**O**	**Si**	**C**	**Zr**
wt.-%	1.31	0.18	0.12	0.050	0.14	0.011	0.013	Bal.
Element	**Al**	**Hf**	**W**	**N**	**H**			
ppm	30	57	20	47	8			

2.2. High-temperature water loop experiments: The Pt deposition was carried out within an autoclave, part of a custom-built sophisticated high-temperature water loop [16]. Typically, a long boiling Zircaloy tube comprising an internal cartridge heater (heat flux ~16 W cm^{-2}), a shorter non-boiling Zircaloy tube and stainless steel 304L specimens were exposed together to simulated BWR conditions (without irradiation of the materials) in this autoclave as schematically depicted in Figure 1a.

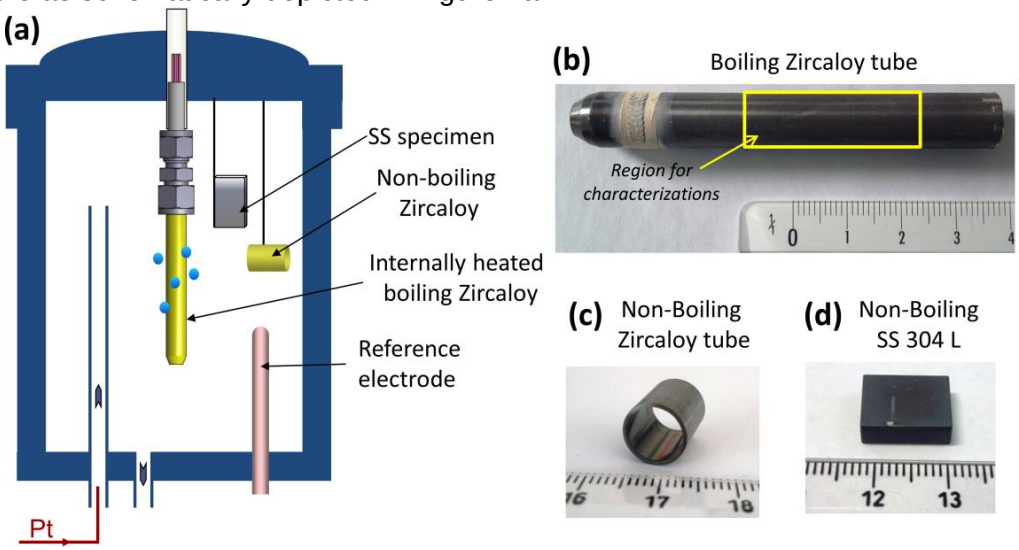

Figure 1. (a) A scheme showing assembly of boiling (symbolized by blue steam bubbles), non-boiling Zircaloy tubes and non-boiling stainless steel 304L specimen for undergoing Pt deposition, and (b-d) corresponding sample pictures post Pt deposition (scale in cm).

The water chemistry can be precisely adjusted in terms of H_2, O_2 and Pt contents. The amount of dissolved H_2 and O_2 gases, water conductivity, pressure, temperature, ECPs and water mass flow were continuously monitored. In this article, results from three tests simulating HWC conditions and lasting 60 days (each) are presented and discussed. They are designated as "No Pt", "Early Pt" and "Late Pt tests. Their test parameters are summarized in Table 2. In order to retain the liquid water throughout the loop, a pressure of ~90 bar was applied. The Pt concentration in the loop water was estimated by knowing the Pt injection rate, Pt concentration of injected solution, and the water flow rate through the autoclave.

Table 2. Summary of test parameters for the three tests.

Experiment designation →	**"No Pt"**	**"Early Pt"**	**"Late Pt"**
Pressure [bar]	89	88	89
T autoclave [°C]	280	280	280
Water mass flow rate [kg/h]	10	10	10
Pt conc. of injection solution [ppb]	n/a	112	105
Pt injection rate [µg/h]	n/a	2.3	2.2
Nominal Pt conc. in water [ppt]	n/a	234	220
Total Pt injected [µg]	n/a	672.5	633.2

In the “No Pt” test, a Zircaloy tube was boiling for 60 days in 280 °C water, without any Pt deposition, and will evidently undergo oxidation. This oxidation phase without having any Pt on the surfaces is referred to, in this context, as pre-oxidation phase. This test serves as a reference. In the “Early Pt” test, keeping the same conditions as “No Pt” test, with the exception that Pt injection was carried out as soon as the loop was stable (thermally and water chemistry, i.e. about 24 h after start of heating). The Pt was injected at a rate of 2.3 μg/h for 10 days, followed by 50 days of post-oxidation phase (referring to oxidation after Pt injection period) and eventually cooled and shut down on the 60th day. While in the “Late Pt” test, Pt injection was started after ~25 days since the inception of heating, at an injection rate of 2.2 μg/h for 10 days, followed by 25 days post-oxidation phase and subsequently cooled and shut down on the 60th day. The timelines of these three tests are sketched in Figure 2. Pictures of boiling Zircaloy, non-boiling Zircaloy tubes and SS 304L specimens after the Pt application from the “Early Pt” test are presented in Figure 1b, 1c and 1d, respectively.

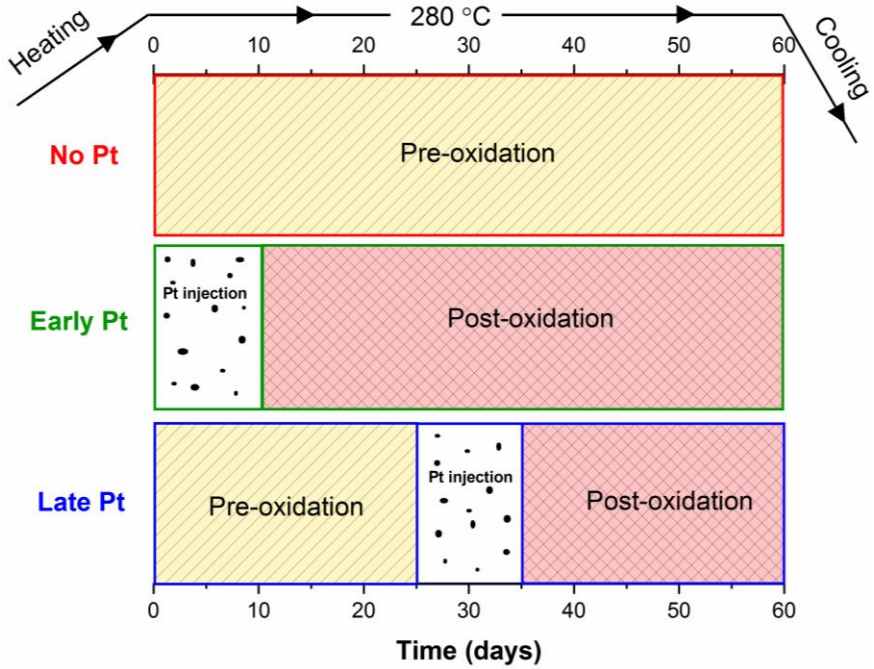

Figure 2. Schematic timelines of the Pt application, pre-oxidation and post-oxidation phases of the “No Pt”, “Early Pt” and “Late Pt” tests in HWC conditions.

2.3. Post-test characterizations: The boiling Zircaloy tubes were first cut lengthwise to remove the cartridge heater. The partially sectioned boiling tube and non-boiling tubes were segmented into several parts for determining the Pt particles’ morphology, sizes and spatial distributions, and Zircaloy oxide morphology and thicknesses. Utmost care was taken to prevent damage of the surfaces either by overheating during the sawing procedure (manually or by a tool) or due to handling. For determining the oxide thickness at the outer diameter of the Zircaloy tubes, cross-sections were embedded in a phenolic resin (KonductoMet^{TM}, Buehler). The embedding was carried out at 290 bar, 150 °C and holding time of 1.5 min. Subsequently, the embedded samples were ground with 180 and 1200 grit SiC emery sheets, and polished with diamond slurries containing 9, 6, 3, 1 and 0.25 μm particles, each for 10 min using 150 N normal load and 150 rpm speed.

A *ZEISS ULTRA 55* scanning electron microscope (SEM) was utilized to investigate the microstructural properties. In-lens or secondary electron (SE) modes were used to characterize the oxide morphology and determining thickness. For obtaining energy dispersive X-ray spectroscopy (EDS) mappings at the oxide-substrate interface, the samples were coated with very thin (few nanometers) carbon films in Baltec MED010 (Switzerland).

The Pt particles were examined in the back scattered electron (BSE) mode exhibiting a high phase contrast with the underlying oxidized surfaces of Zircaloy and stainless steel due to significantly different "Z" values. Since the practical resolution limit of this SEM is ~3 nm, the Pt particles smaller than this limit could not be detected and thus not studied here.

The hydrogen contents in the Zircaloy specimens were determined by hot gas extraction method using the hydrogen analyser *ROH-600,* from *LECO* (*Saint Joseph, MI, USA*), which comprises an electrode oven for heating. After outgassing, the graphite crucibles are loaded with the weighed (~100-200 mg) Zircaloy samples. The temporal release of the H_2 gas occurs firstly from the oxide layer and then from the Zircaloy alloy due to step-wise increase of the electrode's heating power that influences the temperature reached by the material. The released H_2 gas is carried by a He stream to an infrared (IR) absorption detector. The integration of the signals over time yields the total hydrogen content in the specimen.

3. Results and discussion

The morphology, size distribution, and surface loadings of deposited Pt nanoparticles will be initially presented. Subsequently, the influence of varying Pt deposition conditions on the oxidation and hydrogen pickup properties of boiling and non-boiling Zircaloy tubes will be described.

3.1. Pt particles' morphology, size distributions and surface loadings

In Figure 3(a-f), typical low and high magnification BSE images of boiling and non-boiling Zircaloy and stainless steel specimens from "Early Pt" test are shown. Pt has a higher atomic number as compared to the equivalent atomic number of the underlying zirconium oxide or iron oxide and eventually appears as white bright dots. In the case of boiling Zircaloy surface, the centre regions of the tubes, as marked in Figure 1b, were analysed because the cartridge heater is internally located in this region that allows representative boiling conditions. Other sections of the tube are relatively colder and do not exhibit boiling conditions. Pt particles showed heterogeneous distributions for a boiling surface as evident from Figure 3b and c.

In the case of non-boiling Zircaloy and stainless steel, the distributions are rather homogeneous (see Figure 3d-f). Occasionally, there are Ag contaminations in the form of nanoparticles or nanorods (not shown here) that have diameters in the range of 50-100 nm, as evidenced in Figure 3e. Similarly, both boiling and non-boiling Zircaloy specimen surfaces from "Late Pt" test also revealed heterogeneous distributions as displayed in Figure 3g-l. The stainless steel specimen surface of the "Late Pt" test revealed distributions similar to the "Early Pt" test and are therefore not shown. Pt particles seem to deposit preferentially on protruding features atop the relatively smooth zirconium oxide film. This implies that in general, Pt particles are more distant from the oxidised Zircaloy surface, thus possibly minimizing any potential direct effect on its corrosion properties. This corroborates with previous findings, where Pt was observed mainly on the outer crud layer [17].

The average particle sizes (arithmetic mean), mode (majority of the particles have this size), size distributions and surface loadings (mass per unit area) of deposited Pt nanoparticles were obtained by analyzing more than ten 100 kX magnified BSE images with the *ImageJ* software [18]. Figure 4 presents the particle size distributions of all the specimens that underwent Pt deposition and Table 3 presents corresponding average particle sizes. They reveal that all the specimens have similar range of particle sizes and match closely to that expected for similar test conditions [1, 15].

In order to quantify the Pt surface coverage, also termed as surface loadings, a minimum of 11 BSE images of 100 kX magnification have been analyzed with *ImageJ* software to obtain Feret's diameters and area of each BSE image. By assuming a spherical shape of the particles, their volumes in each image can be estimated and eventually the mass of these particles. The surface loading from one BSE image area is simply the ratio of total mass of Pt

particles and the image area. More mathematical models for volume estimations and error analyses are presented elsewhere [19]. Such estimated surface loadings for each specimen are graphically presented in Figure 4 and vary between 50 and 1500 ng/cm^2, with majority of them and corresponding mean values lying between 50 and 500 ng/cm^2. Even though those Pt surface loading values are subject to a rather large error, it can be seen that, as expected, the boiling Zircaloy has a tendency to attract more Pt particles than the non-boiling one and that there are clear demonstrations of heterogeneous distribution of the Pt on the boiling tubes of “Early Pt” and “Late Pt” tests and also non-boiling tube of “Late Pt” tests. This is consistent with the BSE images shown in Figure 3.

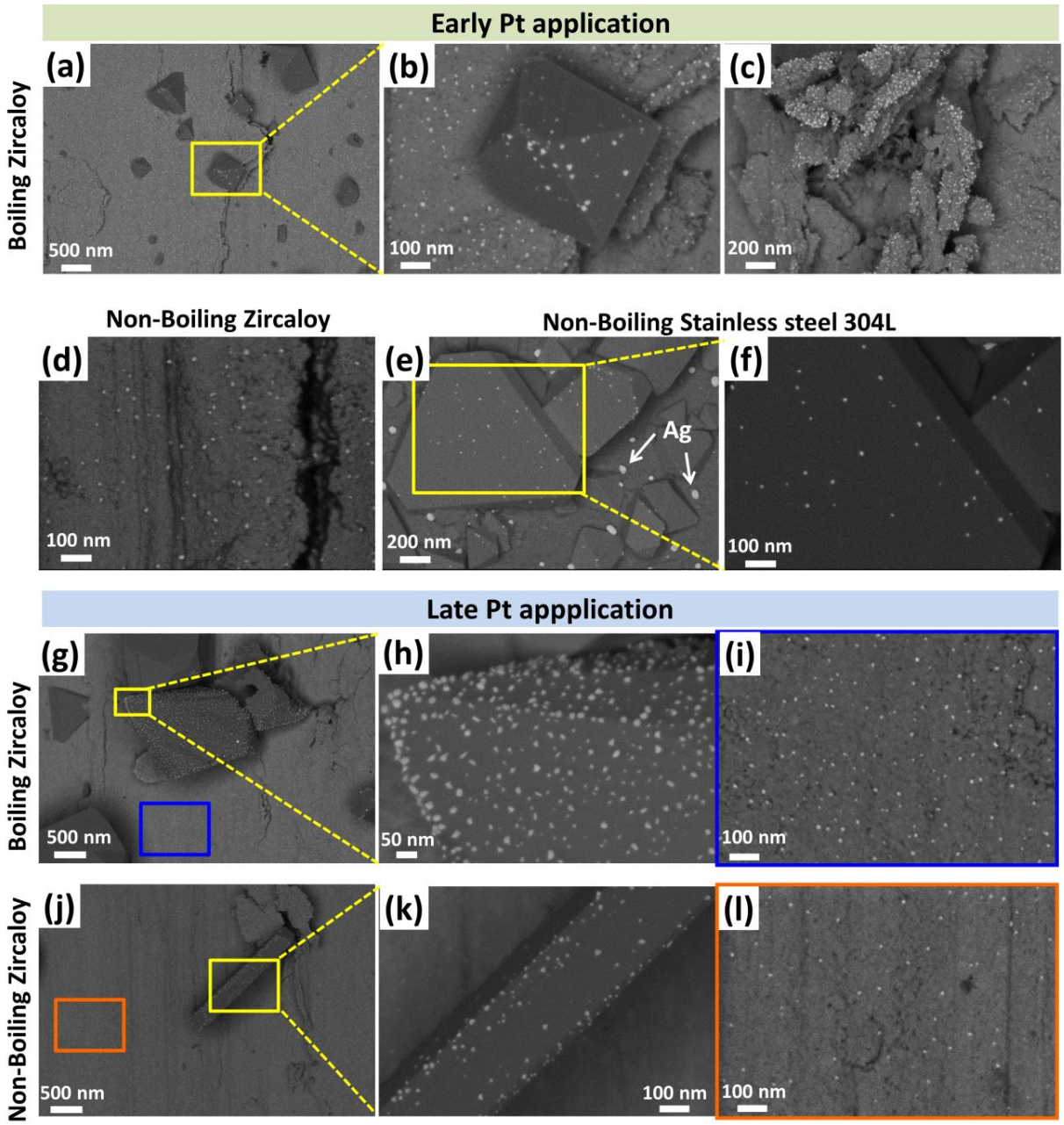

Figure 3. (a-f) Typical low and high magnification BSE-SEM images from “Early Pt” are shown as: (a-c) boiling Zircaloy tube demonstrating heterogeneous distributions of Pt particles, while (d) non-boiling Zircaloy tube and (e-f) stainless steel 304L constitute homogeneous distributions. (g-l) Low and high magnification BSE-SEM images from “Late Pt” test for (g-i) boiling and (j-l) non-boiling Zircaloy tubes demonstrating heterogeneous distributions of Pt particles.

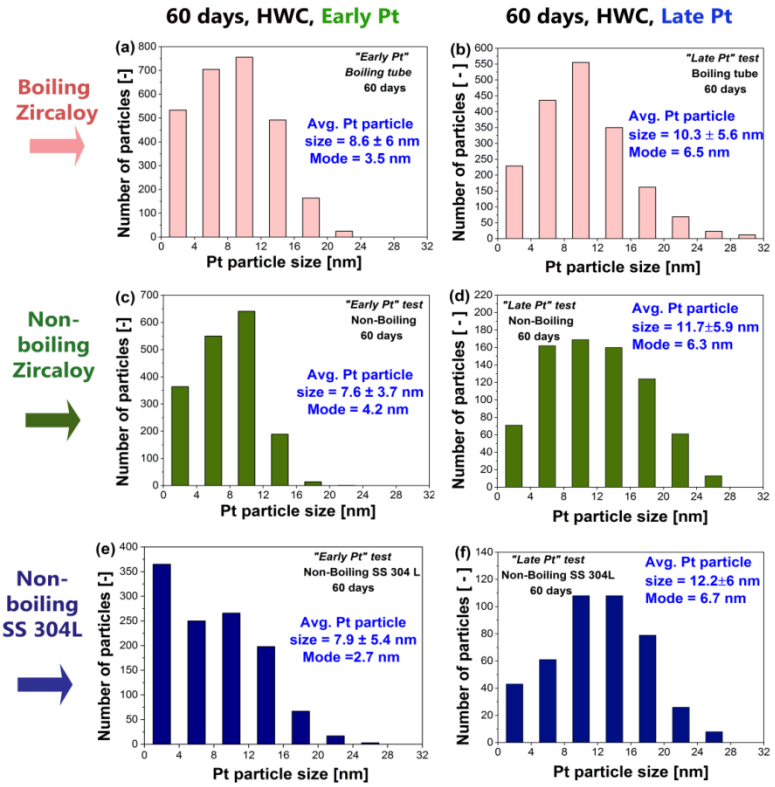

Figure 4. Pt particle size distributions of (a-b) boiling, (c-d) non-boiling Zircaloy tubes and (e-f) stainless steel 304L specimens from "Early Pt" and "Late Pt" tests in hydrogen water chemistry (HWC) conditions, as measured from more than ten BSE-SEM images (≥100 kX magnification).

Table 3. Summary of mean Pt particle sizes (± one σ) of boiling and non-boiling tubes of "Early Pt" and "Late Pt" tests as measured from BSE-SEM images.

Sample description	Mean Pt particle sizes (nm)	Geom. mean Pt particle sizes (nm)	Particle size mode (nm)
Early Pt-Boiling	8.6±6	6.7×/2.2	3.5
Early Pt-Non-Boiling	7.6±3.7	6.4×/1.9	4.2
Early Pt-SS 304 L	7.9±5.4	5.8×/2.3	2.7
Late Pt-Boiling	10.3±5.6	8.5×/2.0	6.5
Late Pt-Non-Boiling	11.7±5.9	9.8×/1.9	6.3
Late Pt-SS 304 L	12.2±6	10.3×/1.9	6.7

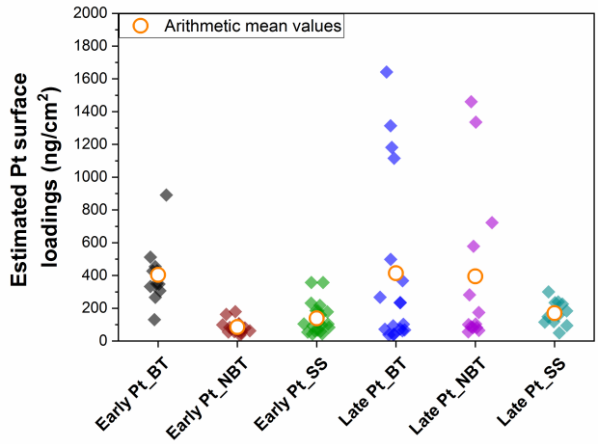

Figure 5. Estimated Pt surface loadings are presented by processing several BSE-SEM images for "Early Pt" and "Late Pt" specimens. Abbreviations in the X-axis title are BT-Boiling Tube, NBT-Non-Boiling Tube and SS-Stainless Steel 304L.

3.2. Oxide morphology

The oxide morphology characteristics of Zircaloy and stainless steel specimens were studied in SEM using SE or InLens detectors. Figure 6a-c shows a compilation of representative SEM images of boiling tubes from “No Pt”, “Early Pt” and “Late Pt” tests. All of them show similar surface microstructure. For example, they have many large iron oxide crystals which crystallized out of the water similar to the outer oxide layer on stainless steel [10]. Since the “Early Pt” test stands for conditions that would be more critical for nuclear power plants, the low, medium and high magnification SEM images of its boiling and non-boiling Zircaloy surfaces are presented in Figure 6d-h. It can be observed that there is a nano-roughened surface film due to oxidation of Zircaloy substrate that constitutes nano oxide grains as shown in Figure 6f,i. Overall, the oxide morphology are comparable to that of Zircaloy specimens that were subjected to 25 days of BWR conditions [15]. On the contrary, the stainless steel specimens contain only densely distributed large iron oxide crystals (not shown here).

3.3. Oxide thickness

As-received Zircaloy specimens exhibited negligible oxidation at room temperature as showcased in Figure 7a, while the specimens exposed to BWR conditions underwent significant oxidation. For example, the strong phase contrast already visible in SE mode for a boiling tube of the “Early Pt” test in Figure 7b clearly shows oxide formation. To verify the resulting contrast, EDS mappings were carried out at this interface revealing a zirconium- and oxygen-rich interface as displayed in Figure 7(c). More than 50 measurements were performed to determine the average oxide thicknesses for all boiling and non-boiling Zircaloy tubes from the “No Pt”, “Early Pt” and “Late Pt” tests, which are graphically summarized in Figure 8. The oxide thicknesses range between 650 and 1400 nm and no detrimental effects of Pt were observed. The outlying value for the non-boiling tube of “Late Pt” test will need further investigation, but is not of a major concern, because the boiling Zircaloy did not confirm this increase in oxide layer thickness.

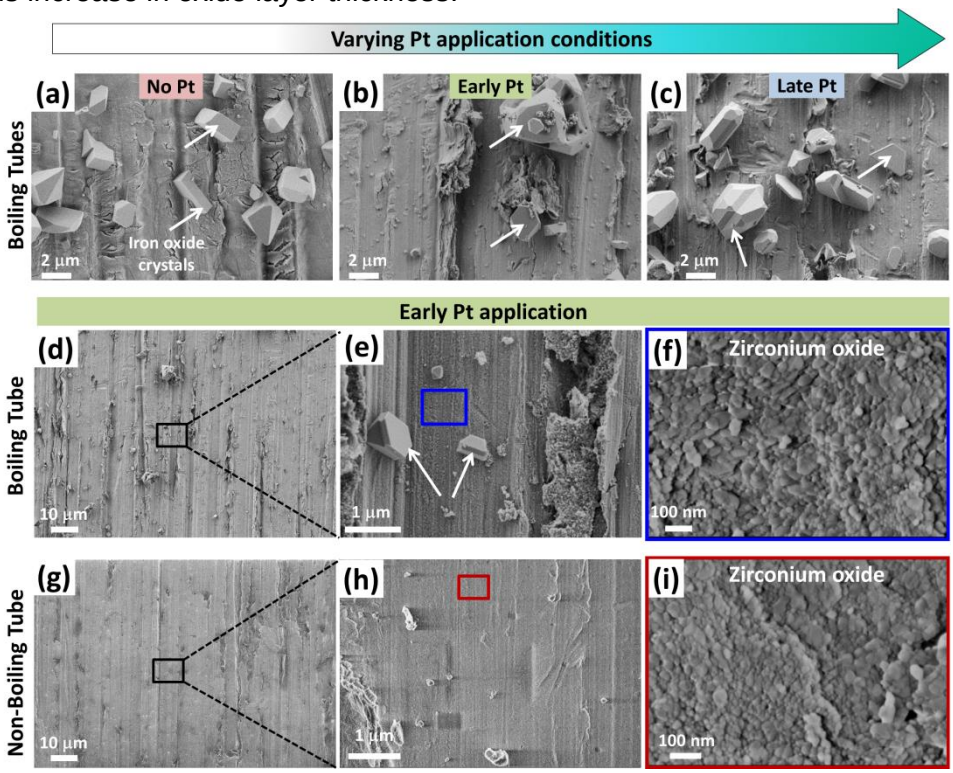

Figure 6. Representative SE-SEM pictures of boiling tubes of (a) “No Pt”, (b) “Early Pt” and (c) “Late Pt” tests showing large iron oxide crystals (white arrows) deposited on the oxidized Zircaloy-2 surfaces. (d-f) Low, medium and high magnification SEM images of boiling tube from “Early Pt” test and (g-h) Low and medium magnification SEM images of non-boiling tube from “Early Pt” test.

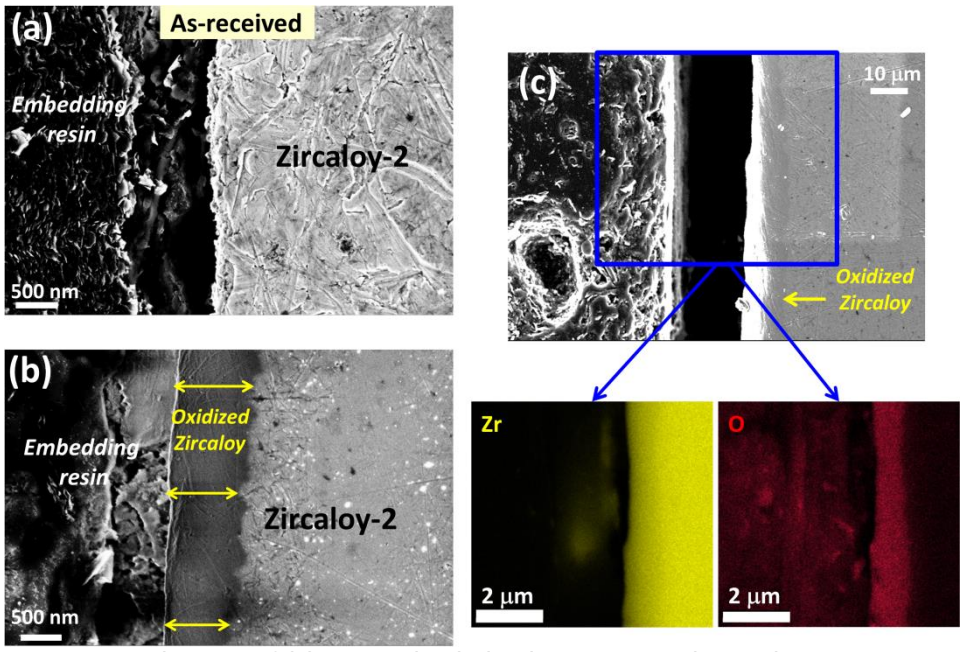

Figure 7. SE-SEM images of (a) as-received Zircaloy cross-section to demonstrate negligible oxidation, (b) boiling tube from "Early Pt" test showing a strong contrast between the zirconium oxide and the Zircaloy substrate, and (c) EDS mappings of the latter specimen to demonstrate the zirconium and oxygen rich interface confirming the oxide.

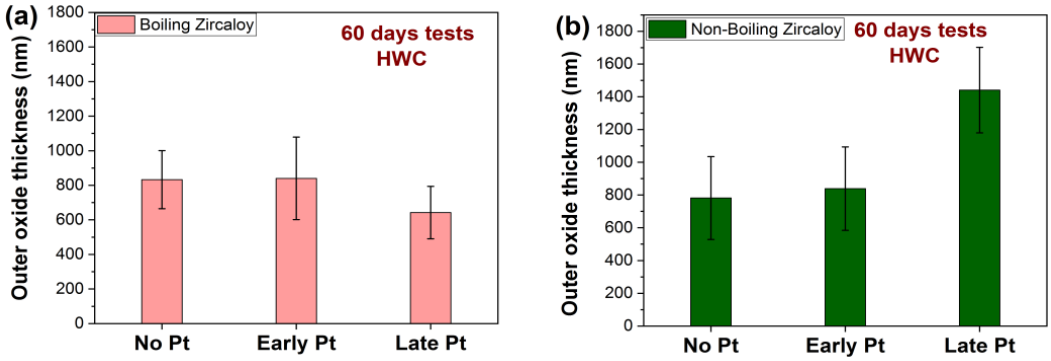

Figure 8. The average zirconium oxide thickness as measured from > 50 values from SE-SEM pictures of (a) boiling, (b) non-boiling Zircaloy tubes from "No Pt", "Early Pt" and "Late Pt" tests.

3.4. Hydrogen content

The hydrogen pickup by Zircaloy alloy is of primary interest, as it can lead to formation of brittle hydrides as inclusions after the solubility limit is exceeded. This will weaken the cladding, leading to possible mechanical failure and unwanted exposure of fuel to the high-temperature water. Hot gas extraction measurements were performed for two samples from each category as wells as for "as-received" tube sections. The average values are shown in Figure 9 for boiling and non-boiling specimens from the "No Pt", "Early Pt" and "Late Pt" tests. The translucent grey overlapping box on the data is the measured hydrogen content from "as-received" material. This value (15 ppm) is slightly higher than that reported in Table 1 (8 ppm), majorly due to several manufacturing steps [20] associated in transforming a Zircaloy-2 ingot into a tube comprising Zircaloy-2 and an inner thin liner. So, the hydrogen content above this base value of 15 ppm corresponds to the influence of the high-temperature water exposure and/or Pt deposition.

Here, it must be noted that the non-boiling Zircaloy tube has both surfaces (outer and inner) exposed to high-temperature water conditions while the boiling tube has only its outer surface exposed (see Figure 1b,c). Therefore, the hydrogen uptake properties must not be

compared one-to-one between the corresponding boiling and non-boiling specimens in this work. It is well-known that the hydrogen uptake properties of this inner liner vary significantly as compared to the rest of the material, as the liner was not primarily designed to withstand corrosion by high-temperature water. Indeed, the formation of a hydride rim has been reported at the liner surface [20]. This may well explain the high hydrogen uptake of the "No Pt" non-boiling (Figure 9b) specimen compared to that of "No Pt" boiling (Figure 9a) specimen. In this context, the lower hydrogen contents of the "Early Pt" and "Late Pt" non-boiling specimens may be surprising at first because the liner of these specimens were also exposed to high-temperature water. However, it may also be an indication that the presence of Pt can inhibit the hydrogen uptake by the liner. This would agree with the claims, made in a patent by General Electric [21, 22], that noble metals are able to reduce the hydrogen absorption in zirconium alloys. Actually the same trend is already present in our previous series of short-term duration experiments [15].

The present data reveals that the increased hydrogen contents (above grey box) are between 2 and 20 ppm. But even the total hydrogen contents (up to 35 ppm) are significantly below the solubility limit (~100 ppm [23]). Importantly, the hydrogen pickup by the Pt-treated samples ("Early Pt" and "Late Pt" tests) are only slightly higher (boiling) or even lower (non-boiling) as compared to their corresponding "No Pt" tests. This clearly suggests that, at least after 60 days, Pt applications have not shown detrimental effects on the hydrogen pickup properties of Zircaloy samples under the presently simulated BWR conditions. But even longer experiments are needed to verify this.

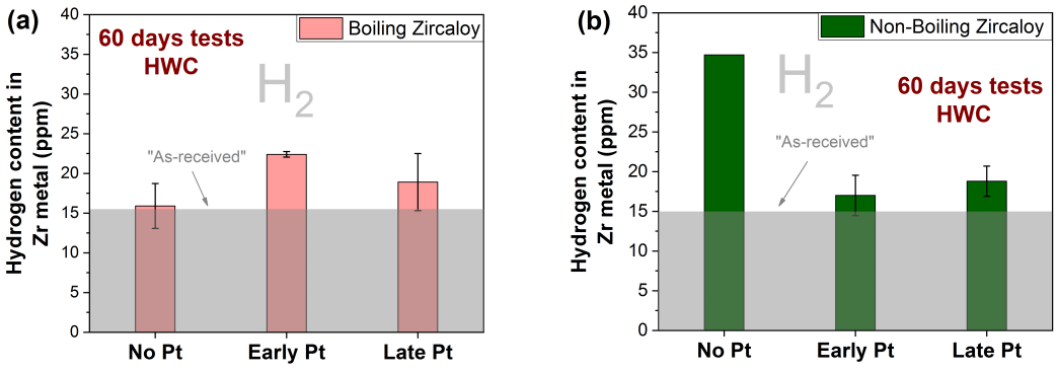

Figure 9. Measured hydrogen contents (in ppm) for (a) boiling and (b) non-boiling Zircaloy specimens from "No Pt", "Early Pt" and "Late Pt" tests are shown. The standard deviation values are resultant of two measurements for each condition. The grey translucent boxes in both the graphs indicate measured hydrogen content of "as-received" specimens without exposure to autoclave as a reference.

4. Conclusions and outlook

This study demonstrates that, at least for 60 days tests, both boiling and non-boiling Zircaloy-2 tubes have not experienced any major detrimental effects in terms of oxidation and hydrogen pickup properties due to deposition of Pt nanoparticles under simulated BWR conditions (without irradiation). Further long-term exposure tests are essential to finally exclude any negative side effects of early OLNC applications. Currently it is planned to carry out tests of longer duration, which will represent more closely a real nuclear power plant cycle and may aid towards finding the optimal waiting time for a Pt application after the deposition of fresh fuel elements.

Acknowledgements

We are grateful for the financial support by the Swiss Federal Nuclear Safety Inspectorate (ENSI) and in-kind contributions from the Swiss nuclear power plants KKL and KKM. We also thank Holger Wiese (PSI) for performing the hot gas extraction measurements and Beat Baumgartner (PSI) for his contribution to the experimental set-up.

References

1. Grundler, P.V. and S. Ritter, *Noble Metal Chemical Addition for Mitigation of Stress Corrosion Cracking: Theoretical Insights and Applications.* PowerPlant Chemistry, 2014. **16**(2): p. 76-93.
2. Hoffelner, W., *Materials for Nuclear Plants: From Safe Design to Residual Life Assessments*. 2013, Springer-Verlag London. p. 65-134.
3. Niedrach, L.W., *Effect of Palladium Coatings on the Corrosion Potential of Stainless Steel in High-Temperature Water Containing Dissolved Hydrogen and Oxygen.* Corrosion, 1991. **47**(3): p. 162-169.
4. Andresen, P.L., et al., *Application of catalytic nanoparticles to high temperature water systems to reduce stress corrosion cracking*, U.p. office, Editor. 2004, General Electric Company: USA.
5. Andresen, P.L., et al., *Mitigation of stress corrosion cracking of structural materials exposed to a high temperature water* U.P. Office, Editor. 2007, General Electric Company: USA.
6. Cowan, R.L. *The Mitigation of IGSCC of BWR Internals with Hydrogen Water Chemistry*. in *Water Chemistry of Nuclear Reactor Systems 7*. 1996. BNES.
7. Hettiarachchi, S., et al., *Noble Metal Chemical Addition... from Development to Commercial Application*, in *7th Int. Conference on Nuclear Engineering*. 1999, JSME: Tokyo, Japan.
8. Hettiarachchi, S. and C. Weber, *Water Chemistry Improvements in an Operating Boiling Water Reactor (BWR) and Associated Benefits*, in *Nuclear Plant Chemistry (NPC) Conference*. 2010, CNS: Quebec City, Canada.
9. Oliver, L., et al., *Review of Water Chemistry and Corrosion Products in a NWC Plant Transitioned to Hydrogen Injection and OLNC*, in *Nuclear Plant Chemistry (NPC) Conference*. 2010, CNS: Quebec, Canada.
10. Castelli, R.A., *Chapter 1 - The Corrosion Source*, in *Nuclear Corrosion Modelling*. 2009, Butterworth-Heinemann: Boston. p. 1-31.
11. Anghel, C., et al., *Effects of Pt surface coverage on oxidation of Zr and other materials.* J. ASTM Int., 2008. **5**(2): p. 1-16.
12. Ballinger, R. and P. Stahle, *Influence of Noble Metals on Zircaloy Corrosion at MIT*, K. Edsinger, Editor. 2004, EPRI: Palo Alto, California. p. 64.
13. Anghel, C., G. Hultquist, and M. Limbäck, *Influence of Pt, Fe/Ni/Cr-containing intermetallics and deuterium on the oxidation of Zr-based materials.* Journal of Nuclear Materials, 2005. **340**(2-3): p. 271-283.
14. Garcia, S.E., J.F. Giannelli, and M.L. Jarvis. *BWR chemistry control status: a summary of industry chemistry status relative to the BWR water chemistry guidelines*. in *Nuclear Plant Chemistry (NPC) Conference*. 2010. Quebec City, Canada: CNS.
15. Grundler, P.V., et al., *Influence of Pt Deposition on the Behaviour of Zircaloy Cladding under Boiling Conditions in Simulated BWR Environment* in *20th Nuclear Plant Chemistry (NPC) International Conference*. 2016: Brighton, UK. p. Paper No. 30.
16. Grundler, P.V., L. Veleva, and S. Ritter, *Formation and deposition of platinum nanoparticles under boiling water reactor conditions.* Journal of Nuclear Materials, 2017. **494**: p. 200-210.
17. Oliver, L., et al. *Impact of Long Term Injection of Platinum (HWC/OLNC) on Water Chemistry, Crud Behavior and Platinum Deposition*. in *Nuclear Plant Chemistry (NPC) Conference*. 2014. Sapporo, Japan: Atomic Energy Society of Japan.
18. Collins, T.J., *ImageJ for microscopy.* BioTechniques, 2007. **43**(1): p. 25-30.
19. Rowthu, S., et al., *Non-destructive ways to characterize local and spatial distributions of platinum nanoparticles on boiling water reactor materials* in *21st International Conference on Water Chemistry in Nuclear Reactor Systems*. 2018: San Francisco, USA.
20. Dahlbäck, M., et al., *The Effect of Liner Component Iron Content on Cladding Corrosion, Hydriding, and PCI Resistance.* Journal of ASTM International, 2005. **2**(9): p. 1-23.
21. Hettiarachchi, S. and D.R. Lutz, *Methods of reducing hydrogen absorption in zirconium alloys of nuclear fuel assemblies*, U.S.P. Office, Editor. 2006, General Electric Company: USA.
22. Hettiarachchi, S. and D.R. Lutz, *Methods of reducing hydrogen absorption in zirconium alloys of nuclear fuel assemblies*, E.P. Office, Editor. 2006, General Electric Company: EU.
23. Slattery, G.F., *The terminal solubility of hydrogen in the zirconium/2 at % chromium/0.16 at % iron alloy.* Journal of Nuclear Materials, 1969. **32**(1): p. 30-38.